DEVELOPMENT OF IR-FEL FACILITY FOR ENERGY SCIENCE IN KYOTO UNIVERSITY

Toshiteru Kii, Hideaki Ohgaki, Kai Masuda, Heishun Zen, Satoshi Sasaki, Takumi Shiiyama and Tetsuo Yamazaki

Institute of Advanced Energy, Kyoto University: Gokasyo, Uji, Kyoto, Japan, 611-0011, kii@iae.kyoto-u.ac.jp

An MIR-FEL facility, KU-FEL, has been constructed for application to energy science, making use of wavelength tunability of FEL enabling to enhance the energy conversion efficiency of the biochemical reactions. The FEL system consists of a compact S-band linac and an undulator to generate 4-13 μm FEL. The linac consists of a thermionic rf gun and a 3-m accelerator tube fed by 10 MW and 20 MW rf powers, respectively. Recent progresses such as an rf input pulse-shape control technique against the back-bombardment effect inherent in thermionic rf gun, and a newly developed beam diagnostic method employing a computer tomography technique have enabled successful production of 40 MeV, 40 mA and 4 μsec electron beams so far, leading to the first observation of 9.2 μm spontaneous emission. Further optimization parameters of both the electron beam and the optical cavity are being pursued for an FEL lasing in the near future. Also studied are a new concept of superconducting micro-undulator and a triode themionic rf gun aiming at a drastic reduction of the back-bombardment for extending the compact IR-FEL performance and its application.

I. INTRODUCTION

An IR tunable coherent light source is quite useful tool to study molecular dynamics, because such light can excite a specific stretching bonds, such as C=N, C=O, Si-H etc which are interesting for production of renewable energy ; i.e. production of alcohol or hydrogen, development of a new type of solar cell, and so on. Thus, in the Institute of Advanced Energy, Kyoto University, we are developing an MIR-FEL (Free Electron Laser) facility. Furthermore, we are thinking such a useful IR source should be widely used for energy science in many laboratories, or companies, thus we are concentrating to establish a compact, economical, and easy-to-operate FEL facility.

II. FACILITY DESIGN

The FEL system is located in the Laboratory for Photon and Charged Particle Research, Institute of Advanced Energy, Kyoto University.

A schematic drawing of the FEL facility is shown in fig. 1. Total area of the facility is 350 m^2 including a klystron gallery and a minimum users' experimental space. Space for accelerator is about 90 m^2, which is almost minimum size to install a 40 MeV linac, beam transport and undulator. Experimental hall for FEL users will be extended in the future.

To reduce a construction cost, height of a radiation shielding wall made of concrete is limited to 2.5 m and stairs is used to access to the accelerator room instead of an expensive shielding door. Part of the shielding wall consists of cubic concrete blocks of 1 m^3 which can be moved to install large devices in the accelerator room.

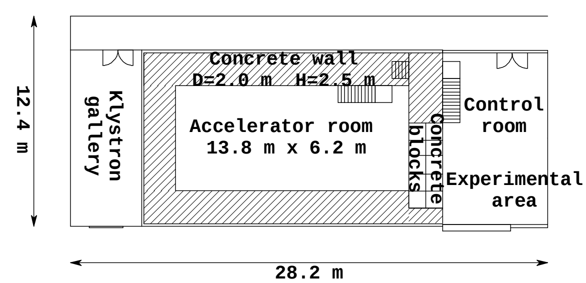

Fig. 1 A schematic drawing of the KU-FEL facility.

III. KU-FEL SYSTEM

The FEL system consists of a 4.5 cell thermionic rf gun driven by a 10 MW klystron, a 3 m accelerator tube driven by a 20 MW klystron, beam transport system, and a Halbach type undulator of 1.6 m. Fig. 2 shows a schematic drawing of the system. An electron beam is accelerated up to 40 MeV by the linac and injected to the undulator. The FEL wavelength from 4 to 13 μm is expected with electron-beam energy from 20 to 40 MeV.

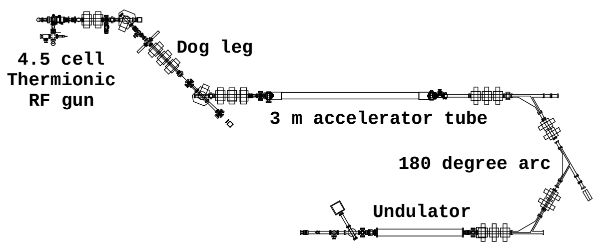

Fig. 2 Arrangement of the KU-FEL.

An S-band thermionic rf gun of 4.5 cells driven by 10MW klystron is used as electron injector in the KU-FEL facility. Transverse magnetic field [1] of about 10 Gauss on the cathode surface is applied to divert back-streaming electrons. Amplitude of the magnetic field is chosen so that transverse kick to the accelerated electron is smaller than the aperture size of the rf gun of 8 mm and a main component of the back-streaming electron of smaller than 300 keV is diverted well. [2] Although the transverse magnetic field can reduce the influence due to the back-streaming electrons, cathode surface temperature increases during macro-pulse duration of several micro seconds. Thus we apply amplitude modulated rf pulse to the rf gun to compensate energy degradation due to back-streaming electrons. [3]

An achromatic transport system (dog-leg section) is comprised of an energy analyzer which consists of a 45-degree bending magnet and a horizontal slit, following 3 quadrupole magnets and another dipole magnet. [4]

An S-band accelerator tube accelerates an electron beam up to 40 MeV by using 20 MW rf power.

A 180-degree arc section was designed for the bunch compressor to obtain high peak current of the electron beam. As seen in fig. 2, this arc section consists of 3 bending magnets and 2 sets of quadrupoles for achromatic condition and for dispersion control to optimize the beam transfer matrix element, R56. Here, the value of the R56 was determined by the energy-phase correlation parameter, $dE/d\phi$, to minimize the bunch length. Two triplet quadrupoles located at both sides of the 180-degree arc work as a beta-match component between the linac and the undulator. [5]

A planar type undulator, which was used for the first lasing experiments under collaboration of the FELI and the University Tokyo [6], is used. The undulator was modified from a fixed gap to a variable gap for easy handling in practical use.

IV. PRESENT STATUS

The beam commissioning was almost finished by the end of Mar. 2007. An electron beam of 9 MeV was successfully extracted from the rf gun, and of 40 MeV was obtained at the exit of the undulator. We will describe our recent studies to achieve the first lasing in our FEL system. .

IV.A. Thermionic rf gun

A thermionic rf gun is a key device for constructing an economical and compact FEL facility, because it does not need any expensive multi-bunched stable short pulse laser or an additional electron beam buncher. However, a serious problem of the back-bombardment limits macro-pulse duration up to several microseconds. The back-bombardment problem is described as follows. Some electrons emitted from the thermionic cathode escaping from the acceleration phase change their direction in the rf gun. And the cathode surface temperature increased due to bombardment of the back-streaming electrons during rf power was stored in the gun. As a result, the number of extracted electron increases, and the beam loading increases. Then the beam energy decreases. So, the electron beam energy is not kept as constant. Typically, in case for our 4.5 cell thermionic rf gun, maximum pulse duration which can pass the 'dog-leg' section was less than 1 μsec.

In order to keep the extracted beam energy as constant, we fed amplitude modulated rf pulse to the rf gun to compensate the energy drop. The rf pulse fed into the rf gun is controlled by remotely adjusting the reactors in the pulse forming network with stepping motors. The effect of the modulated rf input was evaluated experimentally.

Fig. 3 shows the experimental setup. A dispenser cathode of 6 mm in diameter is mounted in the first half cell of the 4.5 cell rf gun. The electron beam current was measured with current transformers (CT) and Faraday cups (FC). The energy spectrum of the electron beam was analyzed with a bending magnet, beam slit and CT2.

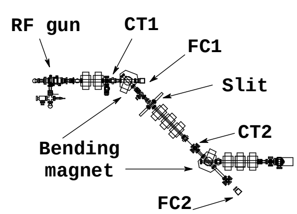

Fig. 3 Experimental setup for the measurement of the beam properties of the energy compensated electron beam.

The experiments have been carried out for modulated rf input pulse. We have succeeded in keeping the peak energy of the electron beam constant in 5 μsec by feeding a modulated rf power into a rf gun. Fig. 4 shows the modulated rf power waveform fed into the rf gun. Fig. 5 shows the beam current waveform whose peak energy is 8.4 MeV at CT2. Fig. 6 shows the time evolution of the peak energy in macro pulse duration.

As shown in fig. 5 feeding the modulated rf power into the rf gun was an effective way to extend the macro pulse duration and to increase the beam current. As shown in fig. 6 the beam energy was kept constant by feeding modulated rf power.

In order to confirm the validity of this method, reflecting rf power waveform was calculated using a equivalent circuit model. Experimental and calculation results agreed well. And also it was found that the degradation of the peak energy could be kept below 100 keV in the macro pulse duration of 8.0 μsec when a proper waveform of the rf power was fed into the rf gun. [3]

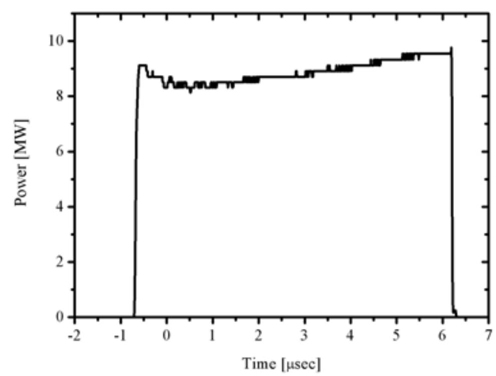

Fig. 4 Waveform of the amplitude modulated rf power fed to the rf gun

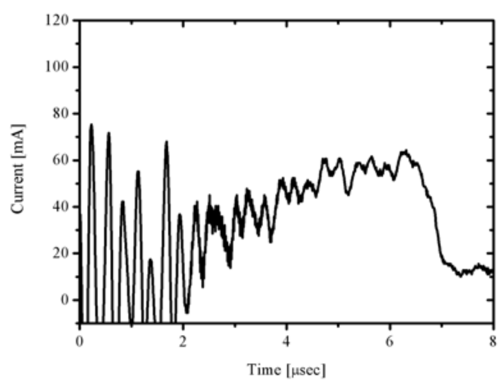

Fig. 5 Beam current measured with CT2

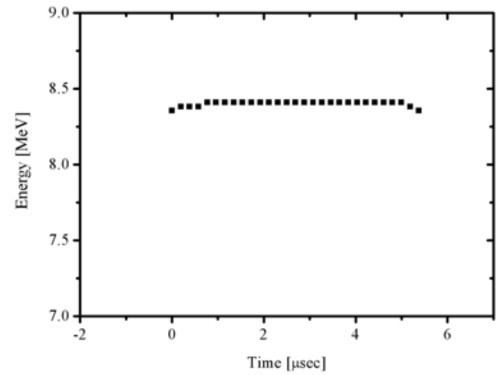

Fig. 6 Measured time evolution of the peak beam energy for the amplitude modulated rf input

IV.B. Electron beam properties with tomographic method

To estimate the expected FEL gain and to put the beam into the best for the FEL experiment, the beam diagnostic is essential. A transverse phase space tomography using a set of a quadrupole magnet and a beam profile monitor is useful method to measure phase space distribution of an electron beam of non-Gaussian space distribution. However, the energy distribution of the measured beam distorts the result of the tomographic method, since the assumption of a mono-energetic beam is required to analyze the phase space distribution using this method. Then we have studied the effect of the energy distribution on the transverse phase space tomography, because an extracted beam from a thermionic rf gun has a low energy tail. Fig. 7 shows the experimental setup. The beam profile monitors (BPM) are consisted of a fluorescence screen (Cr doped Al_2O_3) and a CCD camera, and its spatial resolutions were 0.05 mm. The dog-leg section in fig. 7 worked as an energy filter and its energy acceptance was about 5%. The quadrupole magnet 1 (Q1) and the BPM1 were used to measure the phase space distributions at the upstream of the energy filter, and Q6 and BPM3 were used to measure them at the downstream. The energy distribution of the electron beam is shown in fig. 8. Unfortunately the electrical signals of the low energy tail (less than 7 MeV) measured by the FC2 were hidden by a background noise. For the tomographic reconstruction, we used the Ordered-Subset Expectation Maximization algorithm [7] whose advantage was that there was no artefact on the reconstructed images.

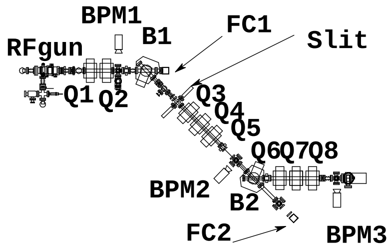

Fig.7 Experimental setup for the analysis of the phase space distribution of the electron beam.

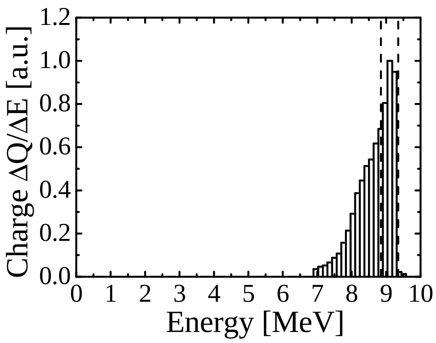

Fig. 8 Energy distribution of the electron beam from the rf gun measured using B1, slit and FC2.

The results of the experiments are shown in fig. 9 (a) at the entrance of Q1 and (b) that of Q6. There are weak and scattered signals in (a) where the electron beam had a low energy tail, but such signals are not seen in (b). Consequently, the signals from low energy tail are reconstructed as weak and scattered signals. The emittances at Q1 and Q6 are calculated as 82 and 12 π mm mrad, respectively. This huge difference comes from the scattering signals in the reconstructed image in Q1.

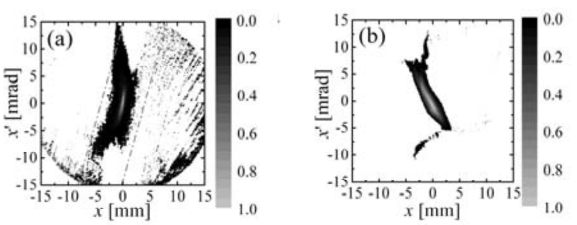

Fig. 9 Phase space distribution at the entrance of Q1 (a) and Q6 (b).

To remove the weak signals produced by the low energy electrons automatically, we introduced an iterative elliptical analysis (IEA) [8]. The procedure is followings:

I : Calculate $\langle x^2 \rangle$, $\langle x'^2 \rangle$ and $\langle xx' \rangle$ from reconstructed phase space distribution.

II : Draw an ellipse defined by eq. 1 on reconstructed phase space.

$$\langle x'^2 \rangle x^2 + 2\langle xx' \rangle xx' + \langle x^2 \rangle x'^2 = 9\varepsilon^2 \quad (1)$$

III: Calculate $\langle x^2 \rangle$, $\langle x'^2 \rangle$ and $\langle xx' \rangle$ from reconstructed phase space distribution only in the ellipse.

IV : In the same way with step II and III, draw an ellipse using newly calculated $\langle x^2 \rangle$, $\langle x'^2 \rangle$ and $\langle xx' \rangle$ in step

V : Repeat step III and IV until $\langle x^2 \rangle$, $\langle x'^2 \rangle$ and $\langle xx' \rangle$ sufficiently converge.

This method was applied to experimental results at the entrance of Q1 and the results are shown in fig. 10. A centre core of reconstructed phase space distribution was successfully extracted and beam parameters were sufficiently converged. As results of application of the IEA, measured emittances of horizontal directions was 5.4 π mm mrad. For equivalent comparison, the IEA was also applied to experimental results at the Q6 entrance and measured emittances of horizontal directions at the Q6 entrance was 7.4 π mm mrad. Taking into account the mismatching condition in the 'dog-leg' section, the emittance at Q1 is reasonable one. Consequently, reliability and an ability of the IEA were shown both in simulation and in experiment.

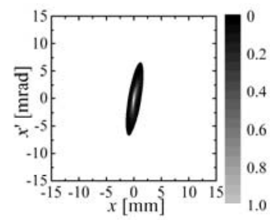

Fig. 10 Phase space distribution with the IEA method at the entrance of Q1.

IV.C. Undulator

The Halbach type undulator has been installed to the FEL system. The undulator length is 1.6 m, the period is 40 mm, the number of period is 40, and the undulator parameter, K-value, is 0.99 ~ 0.17. The magnetic field of the undulator was measured in vertical and horizontal direction using a Hall probe manufactured by F. W. BELL. The probe was driven by a moving stage which was moved on the central axis of the undulator by 1 mm step using a stepping motor. The measured magnetic field of the undulator is shown in fig. 11. Fig. 11 clearly shows demagnetization in the downstream part, peak number 70-78.

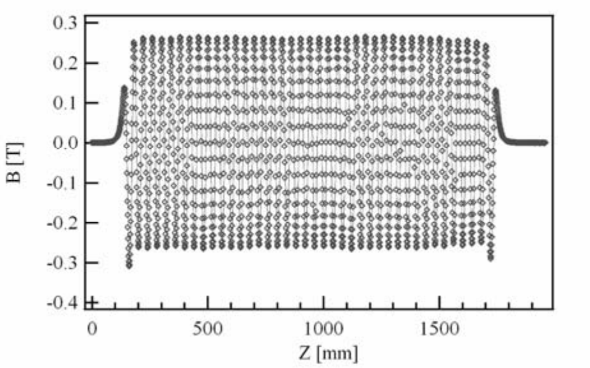

Fig. 11 Measured magnetic field of the undulator along the electron beam axis.

An evaluation of the beam trajectory and spontaneous radiation is an effective method to verify the measurement of the magnetic field. Thus we calculated the electron beam trajectories at 30 MeV with the measured magnetic field and the designed field by using SRW [9]. It was found that the vertical displacement of the electron beam in the undulator can be corrected using a steering magnet as shown in fig. 12. The radiation intensity calculated from the measured magnetic field is reduced by 9 %, and the spectrum is shifted to longer wavelength, compared with that from the design field as shown in fig. 13.

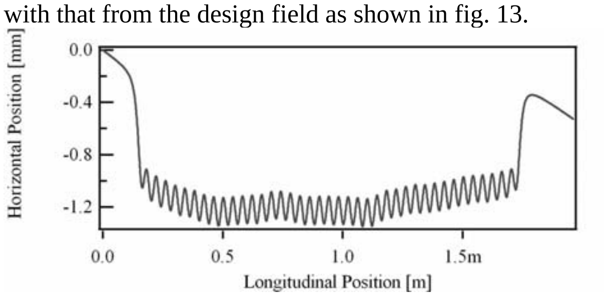

Fig. 12 Horizontal trajectories calculated from the measurement with deflection by the steering magnet located at the entrance of the undulator.

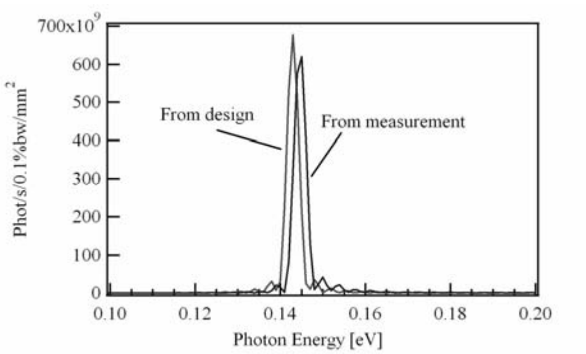

Fig. 13 Calculated spectra of the spontaneous radiation for the designed and the measured magnetic field.

Spontaneous radiation was successfully observed in Dec. 2006. Fig. 14 shows an experimental setup for the spectrum measurement. The optical resonator, a monochromator : DK240 (Digikrom Inc.) and an InSb IR detector : J15D12 (Judson Inc.) were aligned using a semiconductor laser. The electron beam trajectory was carefully controlled to optimize strength of the spontaneous radiation using the beam profile monitors and the steering magnets.

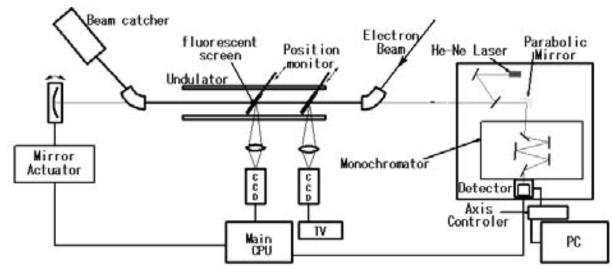

Fig. 14 Experimental setup for the measurement of the spontaneous radiation

The spectra measurement was carried out for the electron beam of 29.5 MeV and the undulator gap of 25.5 mm. The measured spectra and the calculated spectra of spontaneous radiation which are given by a simulation code SRW [9] are shown in fig. 15. As shown in fig. 15 spectrum width (FWHM) is about 270 nm at 9200 nm.

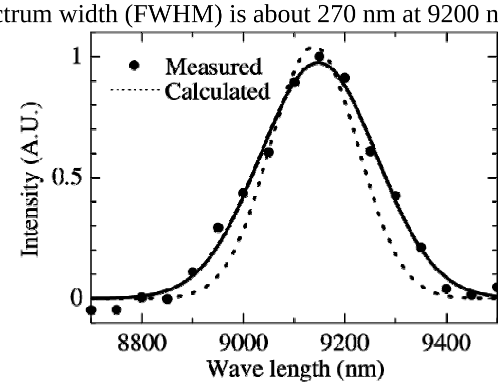

Fig. 15. Measured and calculated spectra of the spontaneous radiation.

IV.D. Estimation of FEL performance

We have calculated FEL gain and saturations to optimize the beam parameter and the optical resonator to obtain the maximum performance of the KU-FEL. The axial symmetric 3D code GENESIS 1.3 [10] was used to calculate the FEL gain and saturation.

The electron beam parameter was optimized by controlling the magnetic field of the 180-degree arc section. Among the electron beam parameters, a peak current (40 A), transverse emittances (11 πmm-mrad in horizontal, 10 πmm-mrad in vertical), and an energy spread (0.5%), which are evaluated by PARMELA [11], are fixed during the calculation. The other electron beam parameters, electron beam sizes and Twiss parameters are optimized to obtain the maximum FEL gain at 25 MeV.

In this work, all the electron beam sizes are RMS values. Twiss parameter α_y is set to zero because the natural focusing of the undulator field is prospective. The parameters of the optical cavity; Rayleigh range and beam waist position, are also optimized to enhance the FEL gain. The optical cavity of the KU-FEL system has been designed taking into account the diffraction loss and the out coupling. The laser field is assumed to be Gaussian in the calculation of the optical loss. The out coupling hole is 2mmϕ located at the upstream mirror. As a result, the curvature of upstream mirror is calculated to be 3.03 m and that of downstream mirror is 1.87 m. The FEL parameters with optimization of both of electron beam and of optical cavity are shown in Table 1.

Table 1 Optimized parameters of the electron beam and the optical cavity to obtain the maximum FEL output.

Beam energy (MeV)	25
Beam size in x (mm)	0.4
Beam size in y (mm)	0.3
Twiss parameter α_x	3.5
Twiss parameter α_y	0
Rayleigh range	0.7 m
Beam waist position	1.1 m
Wavelength (μm)	12.1
Total loss (%)	11.0
Gain of real undulator (%)	37

V. DEVELOPMENT FOR UPGRADE

Several developments have been carried out by our group to improve the MIR-FEL performance.

V.A. Triode thermionic rf gun

An electron beam with a high brightness and high averaged current is preferred for high power FELs. Although a thermionic rf gun is suitable for an economical and compact FEL facility, a serious problem of the back-bombardment limits macro-pulse duration up to several microseconds. Several methods have been proposed to produce an electron beam with long macro-pulse, but the crucial solution has not been developed.

A method has recently been proposed to reduce the back-bombardment using a triode structure driven by rf power, employing a cut-off drift space structure. We investigated the triode-type thermionic rf gun with an additional small cavity (see fig. 16), which is easy to implement as it requires only a modest rf power supply of several tens kW. By use of 1D and 2D particle simulations, we evaluated the reduction of the back-bombardment in a thermionic rf gun using a triode structure. The back-bombardment can be greatly reduced as is shown in Table 2, when an rf power of 30 kW was fed to the triode, though the beam quality is extremely improved in peak current I_{peak}, transverse and longitudinal emittance ε_r and ε_z, brightness B.

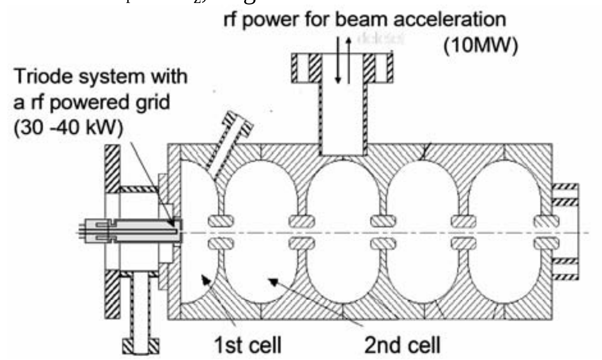

Fig. 16. Concept of the triode thermionic rf gun which have the additional rf cavity at the thermionic cathode.

Table 2 Expected performance of the conventional and the triode thermionic rf gun.

	conventional	Triode
P_{back} [kW]	36	3.6
I_{peak} [A]	17	114
ε_r [πmm· mrad]	2.5	2.0
ε_z [psec MeV]	0.046	0.012
B [A/(πmm· mrad)^2· keV]	0.27	1.6

V.B. New type superconducting micro-undulator

A micro-undulator will be a useful device for a compact FEL device and/or a short wavelength FEL. To realize the micro undulator with undulator parameter K=1 for a period of 5 mm, periodic transverse magnetic field B_0 should be almost 2 T. To obtain strong periodic transverse magnetic field in a short period, we introduce a following high T_c superconducting micro-undulator as shown in fig. 17. [12]

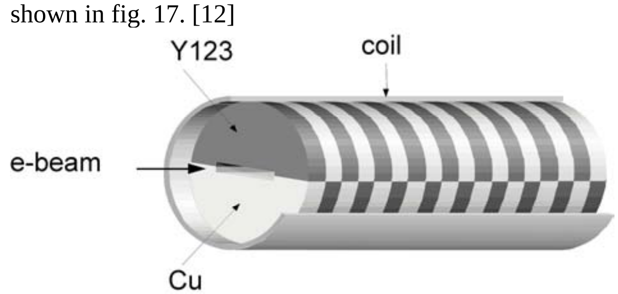

Fig. 17. Conceptual drawing of the high T_C SC undulator. High Tc superconducting materials and nonmagnets are stacked.

Structure and operation of the undulator are as follows. High T_C bulk superconducting materials are stacked in the solenoid. First, these superconducting pieces are cooled down below the critical temperature T_C. Then, the solenoid field is applied. As a result, density modulation of the magnetic field is produced, and thus the periodic transverse magnetic field is generated on the electron beam axis. A preliminary experiment has been performed to confirm the proposed micro-undulator. Preliminary performance was not enough with $YBa_2Cu_3O_7$ (YBCO) ceramic. Further development has been continued to realize a high performance micro undulator.

VI. SUMMARY

We have constructed a compact and economical MIR-FEL facility (KU-FEL) for the “Energy science” using its wavelength tenability in the MIR range at the Institute of Advanced Energy, Kyoto University. The MIR-FEL device has been installed in the Laboratory for Photon and Charged Particle Research. The electron beam was successfully accelerated up to 40 MeV by the linac and injected to the undulator. Spontaneous radiation was observed from a Halbach type undulator in the MIR range. To achieve the first lasing in the KU-FEL system, we have studied on several subjects.

An improvement of the performance of the thermionic rf gun which has a disadvantage of the back-bombardment problem is essential for increasing the FEL gain in the KU-FEL system. We have developed the rf power modulation method to compensate the energy drop due to the back-streaming electrons in the rf gun. Successfully the peak energy of the extracted electron was kept as constant up to 5 μsec. Moreover, the calculation predicts that the degradation of the peak energy of the electron beam could be kept below 100 keV in the macro pulse duration of 8.0 μsec with a proper waveform of the rf input.

A beam diagnostic using a phase space tomography technique has been also studied to estimate the FEL gain and to find the best condition for the FEL experiment. The experimental data shows that the low energy electrons are reconstructed as weak and scattered signals, which would cause an overestimate of the beam emittance. To remove the signals from low energy electrons, an iterative elliptical analysis (IEA) was introduced and applied to the experimental results at the upstream of energy filter and compared with the experimental results at the downstream of the filter. Reliability and ability of the IEA were confirmed from the experiments.

A measurement of the magnetic field of the undulator has been carried out. Although the demagnetization in the downstream part was found, an influence to the strength of the radiation intensity is less than 10%. Also found that the electron beam trajectory could be corrected using the steering magnet. Spontaneous radiation of 9200 nm with spectrum width of 270 nm (FWHM) was successfully observed.

To achieve the first lasing in our FEL system, the beam parameters and the optical parameters were optimized. The FEL gain of about 40 % at 25 MeV was expected with the optimized condition.

Several developments for the upgrade of the FEL performance of the facility have been also carried out. A triode structure driven by rf power of 30 kW was studied to reduce the back-bombardment effect. By use of the particle simulations, it was found that the back-streaming beam power would be greatly reduced and the beam properties would be improved. Design studies on superconducting micro undulator have been also carried out to obtain strong periodic transverse magnetic field in a short period.

ACKNOWLEDGMENTS

This work was supported by the Grant-in-Aid for Young Scientists (A) by the Ministry of Education, Culture, Sports, Science and Technology of Japan.

REFERENCES

1. C.B. MCKEE, et al., Nucl. Instr. And Meth. A **296** ,716 (1990).
2. T. KII, et al., Nucl. Instr. And Meth. A **507** ,340 (2003).
3. T. KII, et al., AIP Conference Proceedings Volume **879**, SYNCHROTRON RADIATION INSTRUMENTATION: Ninth International Conference on Synchrotron Radiation Instrumentation, 248 (2006).
4. K. MASUDA, et al., Proceedings of the 2004 FEL conference, 450 (2004).
5. H. OHGAKI, et al., Proceedings of the 2004 FEL conference, 454 (2004).
6 E. NISHIMURA, et al., Nucl. Istr. and Meth. A **341** 39 (1994).
7 H.M. HUDSON, et al., IEEE. Trans. Med. Imaging, **13**, 601 (1994).
8 H. ZEN, et al., AIP Conference Proceedings Volume **879**, SYNCHROTRON RADIATION INSTRUMENTATION: Ninth International Conference on Synchrotron Radiation Instrumentation, 240 (2006).
9 O. CHUBAR, et al., Proc. of EPAC98, 1177 (1998)
10 S. PEICHE, Nucl. Istr. and Meth. A **429**, 243 (1999)
11 L.M. YOUNG, et al., PARMELA, LA-UR-96-1835, (2001)
12 T. KII, et al., Proceedings of International Conference on Free Electron Laser, 653 (2006).